10.5152/turkjnephrol.2020.3859

Original Article

Turkish Journal of Nephrology

Evaluation of the Parathyroid Gland using Ultrasound Elastography in Children with Mineral Bone Disorder Due to Chronic Kidney Disease

İlknur Girişgen[1], Gülay Güngör[2], Selçuk Yüksel[1]

[1]Division of Pediatric Nephrology, Pamukkale University School of Medicine, Denizli, Turkey
[2]Department of Radiology, Pamukkale University School of Medicine, Denizli, Turkey

Abstract

Objective: Mineral bone disorders due to chronic kidney disease (CKD-MBD) in children occur as a result of decreased glomerular filtration rate and abnormalities in phosphorus, calcium, parathyroid hormone, and vitamin D metabolism rates. Increased parathormone synthesis may result in the development of adenomas in the parathyroid gland. The aim of this study was to evaluate parathyroid lesions in children with CKD-MBD using ultrasound (US) elastography.
Materials and Methods: Fifteen patients with a diagnosis of CKD-MBD (average age, 15.5±2.4 years; seven girls) and 15 healthy children (average age, 13.8±2.5 years; six girls) were included in the study. The patients were evaluated clinically and in terms of laboratory findings (calcium, phosphorus, alkaline phosphatase, vitamin D, and parathormone levels), and all patients were evaluated using strain US elastography. The parathyroid strain ratio indices of the study group were compared with the thyroid strain ratio indices of the control group.
Results: Among 11 patients with stage 5 CKD who underwent parathyroid US, nodules were observed in 8 patients, whereas parathyroid nodules were not observed in 3 patients with stage 3-4 CKD. The parathyroid lesions average strain ratio index (1.1±0.5) was significantly higher than that of the control group (0.46±0.16).
Conclusion: The stiffness of parathyroid lesions in children with US elastography was evaluated for the first time in this study to the best of our knowledge, and it is believed that a high strain ratio index could be a useful indicator of the presence of adenomas. We propose that the findings be supported by future larger studies.
Keywords: Elastography, children, parathyroid gland

Corresponding Author: Selçuk Yüksel ✉ selcukyuksel.nephrology@gmail.com
Received: 21.03.2019 **Accepted:** 18.11.2019

Presented in: This study was presented at the "10th Turkısh Pediatric Nephrology Congress," 1-4 May 2019, Muğla, Turkey.

Cite this article as: Girişgen İ, Güngör G, Yüksel S. Evaluation of the Parathyroid Gland using Ultrasound Elastography in Children with Mineral Bone Disorder Due to Chronic Kidney Disease. Turk J Nephrol 2020; 29(1): 45-51.

INTRODUCTION

Mineral bone disorders in children with chronic kidney disease (CKD-MBD) are caused by abnormal interactions between the kidney, bone, and parathyroid gland, and they are closely associated with cardiovascular morbidity and mortality (1). As the glomerular filtration rate (GFR) decreases, phosphorus excretion in the urine in the early stages and active vitamin D synthesis in the kidney decrease, leading to a decrease in calcium, and the synthesis of secondary FGF-23 and parathormone (PTH) begins to increase. Secondary hyperparathyroidism is clinically called renal osteodystrophy (RO) and is classified into three types according to bone transformation/mineralization. In high bone turnover RO, the osteoblastic and osteoclastic number and cycle increase, the PTH level is high, osteitis fibrosa cystica can be observed, and bone mineralization is normal. In low bone turnover RO (adynamic bone disease, osteomalacia), bone formation is decreased, mineral-free bone tissue is increased, and the PTH level is low. In mixed bone disease, the bone turnover is increased and mineralization is decreased (1, 2). CKD-MBD in children results in bone fractures, skeletal deformities, growth disorders, bone pain, and vascular, metastatic, and soft tissue calcifications (1). Increased

PTH synthesis may result in diffuse or nodular cell growth and development of adenomas in the parathyroid gland. If the hyperplasia of the parathyroid gland is particularly nodular, the development of adenomas is more likely. As a result of the decrease in calcium and vitamin D receptors in the parathyroid gland, the adenoma can become autonomous, and resistance to active vitamin D treatment may develop (3). Tertiary hyperparathyroidism may develop in patients with secondary hyperparathyroidism in whom the parathyriod gland works autonomously which cannot be suppressed by treatment.

Ultrasonography (USG) and ^{99m}Tc Sestamibi (MIBI) scintigraphy are currently the most widely used imaging techniques to detect the location of parathyroid adenomas. The sensitivity of these techniques in identifying parathyroid adenomas is 70%-90%. Although magnetic resonance imaging and 4-D computed tomography have the potential to increase the accuracy of identification, they are expensive (4-7). USG is an inexpensive, noninvasive, and widely used imaging modality to evaluate the parathyroid gland in patients with hyperparathyroidism. However, it may be difficult to differentiate a parathyroid lesion from thyroid nodules or cervical lymph nodes (8, 9).

Currently, elastography, which is a relatively new technique developed by adding software, is based on the general principle that stress applied to the tissues with the help of USG, similar to the palpation technique in physical examination, causes changes in the tissue depending on the elastic properties of the tissue (10). Strain elastography (SE), which is one of the elastography techniques, provides semi-quantitative values of the stiffness of the tissue and the strain ratio (SR) value calculated with the help of software and thus helps to differentiate between tissues and accurately evaluate superficial tissues such as the breasts, prostate, scrotum, neck, and thyroid. If adequate external pressure is applied, adjacent organs such as the parathyroid gland can also be evaluated using this technique (11, 12).

It is well known that the parathyroid gland is normally composed of 40%-70% adipose tissue and that there is a significant decrease in fat content in parathyroid adenomas. In addition, parathyroid adenomas have been shown to have thickened capsules (13, 14). Therefore, parathyroid adenomas are expected to be relatively hard lesions. In recent years, parathyroid lesions have been evaluated using various elastography methods in adults in a limited number of studies. In addition, to the best of our knowledge, although there is a publication evaluating the images of parathyroid lesions using the SE technique in adult patients, no study has been performed using this method in pediatric patients (11).

The aim of this study was to evaluate the appearance of parathyroid lesions in children with secondary hyperparathyroidism caused by CKD by USG and to prospectively determine whether SE can be a valuable additional tool in the diagnosis of parathyroid adenoma.

MATERIALS AND METHODS

The study was prospectively designed to evaluate the parathyroid lesions of 15 children with CKD-MBD using USG elastography. The control group comprised 15 age- and sex-matched healthy children.

Calcium, phosphorus, alkaline phosphatase, vitamin D, and PTH were evaluated in serum samples taken in the morning in routine laboratory tests for BMD. Analyses of biochemical laboratory tests were performed using routine Cobas 8000 series modular autoanalyzers (Roche Diagnostics, Mannheim, Germany). Serum calcium, phosphorus, and alkaline phosphatase levels were measured using the photometric method with a c702 autoanalyzer, and vitamin D and PTH levels were measured using the electrochemiluminescence immunological method with an e601 autoanalyzer.

Radiologically, all patients were evaluated using a conventional B-mode and SE. Axial B-mode and SE images were obtained using a digital sonography device (LOGIQ E9, GE Healthcare, Milwaukee, WI) supported by SE software using 11-15 MHz linear probes to parathyroid glands. All measurements were performed by the same radiologist who had 10 years of experience with USG and 7 years with SE. An USG evaluation was performed using an adequate amount of USG gel. For the measurement of the parathyroid lesion, subjects were laid supine on the examination table in a position with the neck slightly extended. First, B-mode USG was performed, and morphological characteristics (echo pattern, shape, presence of halo sign, and presence of calcification), size, and localization of each lesion were evaluated.

In the second stage, SE was performed immediately after B-mode USG. While the parathyroid images were captured, the SE mode was turned on, and another B-mode image was opened next to the original B-mode image. The local strain was achieved by applying light repetitive compression (rhythmic compression-relaxation cycle) with a free-hand technique while the probe was in the scanning position (15, 16). The SE image was observed as a translucent, color-coded, and real-time image superimposed with the B-mode image. Repetitive compression was continued until more than three SE images were obtained. The hardness of tissues was shown in a color-coded map in which soft tissues were red, hard tissues were blue, and moderately elastic tissues were green (17). Strain elastograms were classified into elastographic patterns according to tissue stiffness (17-20). Figure 1 gives an example of cases with various elastographic patterns. After screening, three SE images were selected randomly during each measurement. In each of the three images, a circular region of interest (ROI) was placed separately into the parathyroid and adjacent thyroid gland. The SR value (B/A) in each ROI was automatically calculated using the USG device by comparing parathyroid (A) to adjacent thyroid (B) for each patient, and the average values were obtained (Figure 2). An SR value was calculated for each of the three images. The average value of the three trials was considered as the SR value

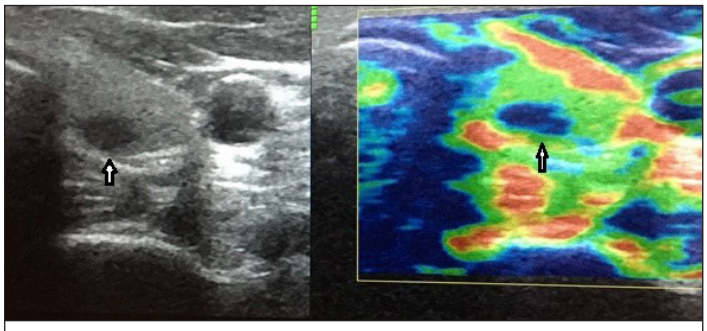

Figure 1. Example of parathyroid adenoma image in conventional ultrasonography (US) and strain elastography (SE). The image on the right shows an oval hypoechoic parathyroid adenoma (arrow) in the inferior neighborhood of the left lobe of the thyroid gland on the gray-scale axial US image. In the picture on the left, Pattern 4 images are seen in SE.

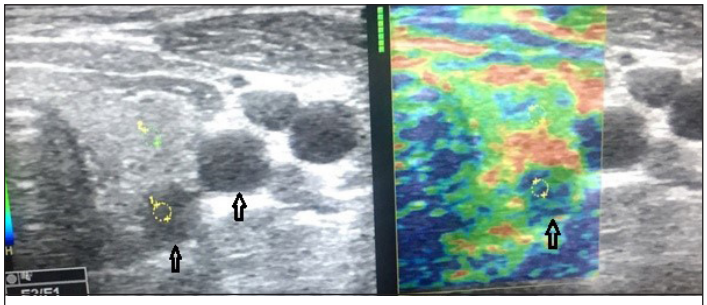

Figure 2. Image of two nodules in the left parathyroid. In the picture on the right, the gray-scale USG shows two well-circumscribed hypoechoic nodules (arrows). The picture on the left shows that the elasticity score of one of the nodules in the SE is consistent with Pattern 4 (arrow). The strain ratio is 0.5.

of each measurement time. The measurements were obtained from only the solid part and noncalcified part of each lesion.

Because normal parathyroid glands are very small, they cannot be evaluated using USG. Therefore, the SR values of the parathyroid gland lesions were compared with the adjacent normal thyroid parenchyma. In the control group, similar measurements were performed for the thyroid gland and compared with the adjacent subcutaneous adipose tissue.

Informed consent was obtained from the families of the patients, and ethics committee approval (19.03.2019/06) was obtained from Pamukkale University medical ethics committee.

Statistical Analysis

Data were analyzed using the The Statistical Package for the Social Sciences (SPSS) version 24.0 package program (IBM Corp.; Armonk, NY, USA). Continuous variables were expressed as the average±standard deviation, and categorical variables were expressed as numbers and percentages. The suitability of the data for normal distribution was examined using the Shapiro-Wilk test. Independent group t-test was used for the analysis of independent group differences, and chi-square analysis was used for the differences between categorical variables. Spearman correlation analysis was used to examine the relationships between continuous variables. In all analyses, $p<0.05$ was considered statistically significant.

RESULTS

The study group comprised 15 laboratory-confirmed patients with CKD-related BMD. The average age of the study group was 15.5±2.4 (12-19) years, and the female-to-male ratio was 7:8. The control group comprised healthy children. The average age was 13.8±2.5 (10-18) years, the female-to-male ratio was 6:9, and there was no significant difference in terms of age and sex between the groups. Demographic and laboratory data and patient treatments are given in Table 1.

The etiologies of patients with CKD were varied, and chronic glomerulonephritis was the most frequently observed etiology (Table 1). Among 15 children with CKD in the study group, 11 had stage 5, 3 had stage 4, and 1 had stage 3 CKD. The dialysis modality of 10 patients with stage 5 CKD was peritoneal dialysis, and one patient was receiving hemodialysis treatment. One patient had a low calcium level, and three had levels >10.2 mg/dL, the target level for that age. The phosphorus level of 13 patients was above the normal limit for that age (>12 years target P level 2.3-4.5 mg/dL [1.21]). Eleven of the 13 patients using active vitamin D had PTH levels more than the target level (PTH target level, 100-300 pg/mL for stage 5 CKD; PTH level, 70-110 pg/mL for stage 3-4 CKD [1.21]). All patients were using calcium-based phosphate binders; 5 were using additional calcium-free phosphate binders (sevelamer), and 13 were on active vitamin D therapy (Table 1).

In the parathyroid USG, nodular lesions (parathyroid adenoma/hyperplasia) were detected in eight patients with stage 5 CKD, whereas three patients had no lesions. No lesions were detected in the patients with stage 3-4 CKD. Table 2 shows the nodule size and SR of the patients with parathyroid nodules. In addition, thyroid nodules were detected using USG in two patients (Table 2). Parathyroid elastography was performed in eight patients with parathyroid lesions in the study group; two patients had pattern 2, one patient had pattern 3, four patients had pattern 4, and one patient with two parathyroid lesions had elastographic patterns 3 and 4. The average parathyroid elastography SR value of the patients with parathyroid lesions in the study group was 1.1±0.5, the average thyroid elastography SR value of the control group was 0.46±0.16, and the average SR value of the study group was significantly high (Table 3).

The presence, size, and SR values of the parathyroid lesion were not correlated with PTH levels.

DISCUSSION

In our study, the parathyroid glands of patients with CKD-BMD were evaluated using USG and elastography. In cases with parathyroid lesions, elastographic features and SR indices were evaluated according to the color score. When compared with the thyroid SR index of the control group, the SR index of para-

Table 1. Demographic, laboratory findings, and treatments of children with bone mineral

Patient Number	Age	Sex	CKD Stage	Primary Disease	Dialysis Modality	Ca	P	ALP	PTH	Vit. D	Ca-based P Binder	Sevalemer	Calcitriol
1	15	M	5	FSGS	PD	9.7	5.1	372	1191	28	+	+	+
2	19	F	5	FSGS	PD	11.3	5.1	56	274	36	+	+	+
3	18	F	5	VUR	PD	9.4	5.7	70	308	46	+	-	+
4	13	F	5	CGN	PD	7.9	5	589	1958	25	+	-	+
5	19	M	5	SLE	PD	8.8	4	142	107	22	+	-	-
6	19	M	5	VUR	PD	9.5	7	68	283	46	+	-	+
7	14	M	5	CGN	PD	7.8	5.5	662	1062	11	+	+	+
8	12	F	5	Neurogenic bladder	PD	10.5	4.4	88	193	29	+	-	-
9	12	F	5	Nephronophthisis	PD	10.8	5.8	188	425	25	+	+	+
10	15	F	5	VUR	PD	9	6.1	283	1738	23	+	-	+
11	14	M	5	VUR	HD	10.1	6.9	819	1500	77	+	+	+
12	14	M	4	FSGS	-	7.6	7.6	129	266	9	+	-	+
13	15	M	3	Nephronophthisis	-	9.7	4.7	246	237	18	+	-	+
14	15	M	4	VUR	-	9.06	4.8	91	217	33	+	-	+
15	19	F	4	IgA nephropathy	-	9.06	5.1	61	242	12	+	-	+

PD: Peritoneal dialysis; HD: Hemodialysis; CKD: Chronic kidney disease; FSGS: Focal segmental glomerulosclerosis; VUR: Vesicoureteral reflux; CGN: Crescentic glomeru- lonephritis; SLE: Systemic lupus erythematosus

Table 2. Ultrasonography and strain elastography results of chil- dren with bone mineral metabolism disorder due to chronic kidney disease

Patient Number	Parathyroid Nodule (mm)	Parathyroid Elastography Strain Ratio	Thyroid Nodule (mm)
1	4x2.5	1.6	-
2	11x10	2.1	-
3	3x3	0.9	-
4	4.5x2.5	0.8	-
5	Absent	-	-
6	Absent	-	-
7	4.7x2.4	1.2	3x2
8	Absent	-	-
9	4.8x2.1	0.8	-
10	5.7x3.6	1	-
11	10.6x10.2	0.5	-
12	Absent	-	8.5x4
13	Absent	-	-
14	Absent	-	-
15	Absent	-	-

thyroid lesions was found to be higher. One of the main findings of this study was that the parathyroid lesions (adenoma/hyperplasia) were very hard masses. It was also thought that SR index elevation may be an indicator of adenoma in patients with parathyroid lesions.

K-DIGO defined CKD-BMD as the presence of one or more of the following findings (21, 22):

Impairment in Ca, P, vitamin D, and PTH metabolism rates

Abnormalities in bone turnover and mineralization and linear bone growth

Calcification in vascular or other soft tissues

Generally, at stage 2 CKD, i.e., a GFR of <90 mL/min/1.73 m^2, laboratory findings of BMD start to emerge (21). Clinically, bone pain, skeletal deformities such as genu valgum, genu varum, fractures, growth retardation, and non-bone vascular and soft tissue calcifications, and myopathy can be observed (21). In addition to laboratory findings, bone marrow biopsy is used to evaluate bone turnover (osteoblastic-osteoclast activity), and bone densitometry is used to evaluate bone mineralization in some cases (22).

In the treatment, phosphorus restriction is made by maintaining phosphorus within normal limits according to age (1-23). Calcium is maintained within normal limits according to age. Phosphorus-binding agents (calcium-containing and non-calcium-containing sevelamer) and active vitamin D-calcitriol to lower the PTH level are used. The target PTH level in children

Table 3. Comparison of the parathyroid elastography parameters of the study group and the thyroid elastography parameters of the control group

	Study Group n=14	Control Group n=15	p
Age (year)	15.2±2.4 (12-19)	13.8±2.5 (10-18)	0.14
Sex (F/M)	7/8	6/9	0.8
Parathyroid nodule elastography (strain ratio index)	1.1±0.5	0.46±0.16	0.009

with stage 5 CKD in the pediatric age group is recommended to be maintained between 100 and 300 pg/mL, and when this level is >500 pg/mL, growth is impaired and the incidence of osteitis fibrosa cystica increases, whereas the risk of hypercalcemia occurs when the level is <100 pg/mL (1,21). If the PTH level exceeds 1000 pg/mL, subtotal parathyroidectomy should be considered when there is no response to vitamin D treatment (vitamin D and Ca receptor levels of the nodular compartment developing in the hyperplastic gland in parathyroid are decreasing), and calcification and calciphylaxis in soft tissues occur. All our patients were receiving phosphorus-restricted diet and calcium-containing phosphorus-binding and active vitamin D therapy, and five patients were receiving additional sevelamer therapy. Despite these treatments, five patients had a PTH level of 1000 pg/mL and 11 had a PTH level above the normal level.

USG is the modality of choice for imaging the parathyroid gland in children. The presence of nodules can be demonstrated using USG. Studies have shown that other lesions in the cervical region (thyroid nodules and lymph nodes) can be confused with parathyroid adenomas in terms of location and structure (8, 9, 24). The indications for MIBI scintigraphy are disputable, and this modality is usually not considered for the diagnosis and for determining the location of the lesion. If parathyroidectomy is indicated, it should be performed to show localization of adenoma or if there is suspicion of ectopic adenoma (21, 25). In addition, if thyroid nodules, lymph nodes, and metastatic masses are present, MIBI scintigraphy specificity decreases, and it has disadvantages such as radiation exposure (25). Studies have shown that the sensitivity of MIBI in hyperparathyroidism is 50%-85%, and at the same time, its sensitivity for the detection of nodules <1 cm decreases further (6, 26).

USG elastography deals with the mechanical properties of the tissue. The hardness of the measured tissue relative to that of neighboring tissues provides information about its consistency. By applying external force, the positional change of the tissue can be examined. The lesser the displacement of a tissue, the greater is the hardness of that tissue. Strain index is obtained by dividing the elasticity ratio of the mass by the elasticity ratio of the healthy adjacent tissue. The first evaluation of the parathyroid gland using the SE method was performed by Ünlütürk et al. (11). It was observed that parathyroid adenomas were hard in SE, and the parathyroid hyperplasias were soft in almost half the cases. The authors found higher SR values and higher elasticity scores (scores 3 and 4) in patients with parathyroid adenoma compared with those with hyperplasia. Similarly, in our study, high elasticity scores and SR values were found in parathyroid lesions. Although the prospective characteristics of the study by Ünlütürk et al. (11) and evaluation in accordance with pathological correlations made positive contributions to the literature, we think that the over-dependency of SE on users is the drawback of the study. There are a considerably fewer number of studies evaluating parathyroid adenomas using elastography. On review of the literature and to the best of our knowledge, there are no studies on this subject in children. After parathyroid adenoma is detected using USG, the SR values calculated when elastography is performed cannot be compared with those of a normal parathyroid gland because normal-sized parathyroid glands are not identified by most imaging methods. Therefore, if the parathyroid gland can be observed on USG, it should be considered a pathological lesion. In our study, parathyroid adenoma SR values were compared with SR values of adjacent tissues, such as the thyroid tissue. In the study by Ioana et al., the parathyroid adenoma SR rates were lower than the thyroid tissue SR rates. However, different results were obtained in different studies. Chandramohan et al. (5) showed that parathyroid adenomas were softer than benign and malignant thyroid nodules, and Batur et al. (27) showed that parathyroid adenomas were more rigid than benign thyroid nodules and less rigid than malignant lesions. In our study, we calculated that the SR values of patients with parathyroid nodules were significantly higher than those of the control group. All patients with parathyroid nodules were stage 5 CKD, and no adenoma was detected in patients with stage 3-4 CKD. In addition, a thyroid nodule was found incidentally on USG in two patients in the study group. Parathyroid adenoma was detected in one of the two patients with thyroid nodules, and reference values in the SR measurements were obtained from localization of normal thyroid parenchyma without thyroid nodules. In other words, lesions observed in the thyroid that could change the reference value did not prevent the evaluation of the parathyroid gland.

The indication for parathyroid scintigraphy is to show the exact localization of adenoma in patients who are considered to require parathyroidectomy because they do not respond to active vitamin D therapy. In our study, parathyroid scintigraphy was performed in one of the patients with secondary hyperparathyroidism (patient 4), whose PTH levels (1958 pg/mL) could not be decreased despite active vitamin D and phosphorus-binding treatments. This patient had suspicious adenoma on USG, and the SR index was 0.8. Parathyroid scintigraphy did not reveal adenoma.

In another patient (patient 2), an adenoma of >1 cm was detected using USG, and the SR index was 2.1, which was considerably high. The PTH level was 274 pg/mL, and parathyroid scintigra-

phy revealed the presence of the adenoma. In the patient (patient 11) with vascular calcification and PTH level of 1500 pg/mL, despite active vitamin D treatment and a 1-cm parathyroid nodule detected on USG, but who had a low SR index (0.5), adenoma was not detected in the scintigraphy performed with the indication of parathyroidectomy. In conclusion, adenoma was not detected in parathyroid scintigraphy in the patient who was resistant to vitamin D therapy, had a PTH level >1000 pg/mL, and a parathyroid nodule >1 cm, but had a low SR index. However, scintigraphy showed an adenoma in the patient whose USG elastography did not show a very high PTH level but had a high SR index.

The data obtained from these three cases suggest that SR, i.e., the elasticity index, in elastography, may be more useful than the increased level of PTH and the size of the adenoma on USG to demonstrate the presence of an adenoma. However, the results from such a small number of patients are insufficient for such a prediction. This finding may serve as a base for larger studies in the future.

CONCLUSION

When we searched the literature, and to the best of our knowledge, there were no similar studies in patients with secondary hyperparathyroidism caused by CKD-BMD, nor was there any study in which the parathyroid gland was evaluated using elastography in children. The first result of our study was that the parathyroid adenomas had higher SR indexes than the thyroid tissue; in other words, they were very hard masses. The second result was that a high SR index may be a good indicator of the presence of adenomas. The limitations of the study are the small number of patients and the inability to detect parathyroid adenomas using parathyroid scintigraphy or parathyroidectomy in all patients. This method was not preferred due to ethical problems. There is a need for studies with more cases and studies compared with parathyroid scintigraphy within the indication.

Ethics Committee Approval: The ethics committee approval was received for this study from the ethics committee of Pamukkale University (19.03.2019/06).

Informed Consent: Written informed consent was obtained from the patients' families who participated in this study.

Peer-review: Externally peer-reviewed.

Author Contributions: Concept - İ.G.; Design - İ.G.; Supervision - S.Y.; Resources - G.G.; Materials - İ.G., G.G.; Data Collection and/or Processing - İ.G., G.G.; Analysis and/or Interpretation - İ.G., S.Y.; Literature Search - İ.G., G.G.; Writing - İ.G., G.G., S.Y.; Critical Reviews - S.Y.

Conflict of Interest: The authors have no conflict of interest to declare.

Financial Disclosure: The authors declare that this study has received no financial support.

REFERENCES

1. Hanudel MR, Salusky IB. Treatment of pediatric chronic kidney disease-mineral and bone disorder. Curr Osteoporos Rep 2017; 15: 198-206. [CrossRef]
2. Kültür T, Çifci A, İnanır A. Bone-minerale metabolism disorders (renal osteodystrophy) in chronic kidney disease and treatment approach. Ortadogu Medical Journal 2016; 8: 214-7.
3. Öncel L. Kronik renal yetmezlikli hastalarda hiperparatiroidizm, tedavi yaklaşımları ve kalsiyum reseptörü allel tiplendirmesi. Haydarpaşa Numune Eğitim ve Araştırma Hastanesi, Doktora tezi. 2017.
4. Johnson NA, Tublin ME, Ogilvie JB. Parathyroid imaging: technique and role in the preoperative evaluation of primary hyperparathyroidism. Am J Roentgenol 2007; 188: 1706-15. [CrossRef]
5. Chandramohan A, Therese M, Abhraham D, Paul TV, Mazhuvanchary PJ. Can ARFI elastography be used to differentiate parathyroid from thyroid lesions? J Endocrinol Invest 2018; 41: 111-9. [CrossRef]
6. Azizi G, Piper K, Keller JM, Mayo ML, Puett D, Earp KM, et al. Shear wave elastography and parathyroid adenoma: A new tool for diagnosing parathyroid adenomas. Eur J Radiol 2016; 85: 1586-93. [CrossRef]
7. Huppert BJ, Reading CC. The parathyroid glands. In:Rumack CM, Wilson SR, Charboneau JW, Levine D eds. Diagnostic Ultrasound, 4th edn, Elsevier Mosby, 2011; pp. 750-69.
8. Polat AV, Ozturk M, Akyuz B, Celenk C, Kefeli M, Polat C. The diagnostic value of shear wave elastography for parathyroid lesions and comparison with cervical lymph nodes. Med Ultrason 2017; 29: 386-91. [CrossRef]
9. Barbaros U, Erbil Y, Salmashoglu A, Işsever H, Aral F, Tunaci M, et al. The characteristics of concomitant thyroid nodules cause false-positive ultrasonography results in primary hyperparathyroidism. Am J Otolaryngol 2009; 30: 239-43. [CrossRef]
10. Menzilcioglu MS, Duymus M, Avcu S. Sonographic elastography of the thyroid gland. Pol J Radiol 2016; 81: 152-6. [CrossRef]
11. Ünlütürk U, Erdoğan MF, Demir O, Culha C, Güllü S, Baskal S. The role of ultrasound elastography in preoperative localization of parathyroid lesions: a new assisting method to preoperative parathyroid ultrasonography. Clin Endocrinol 2012; 76: 492-8. [CrossRef]
12. Garra BS. Imaging and estimation of tissue elasticity by ultrasound. Ultrasound Quarterly 2007; 23: 255-68. [CrossRef]
13. Isidori AM, Cantisani V, Giannetta E, Diacinti D, David E, Forte V, et al. Multiparametric ultrasonography and ultrasound elastography in the differentiation of parathyroid lesions from ectopic thyroid lesions or lymphadenopathies. Endocrine 2017; 57: 335-43. [CrossRef]
14. Herrera MF. Parathyroid embryology, anatomy, and pathology. In: O.H. Clark, Q.Y. Duh, E. Kebebew eds. Textbook of Endocrine Surgery, 2nd edn, Elsevier Saunders, Philadelphia, PA, 2005; pp. 365-71. [CrossRef]
15. Herek D, Herek O, Akbulut M, Ufuk F. Role of strain elastography in the evaluation of testicular torsion: An experimental study. J Ultrasound Med 2016; 35: 2149-58. [CrossRef]
16. Ophir J, Alam SK, Garra B, Kallel F, Konofagou E, Krouskop T, et al. Elastography: ultrasonic estimation and imaging of the elastic properties of tissues. Proc Inst Mech Eng H 1999; 213: 203-33. [CrossRef]
17. Dowell B. Real-time tissue elastography. Ultrasound 2008; 16: 123-7. [CrossRef]
18. Dumitriu D, Dudea S, Botar-Jid C, Baciut M, Baciut G. Real-time sonoelastography of major salivary gland tumors. Am J Roentgenol 2011; 197: 924-30. [CrossRef]

19. Itoh A, Ueno E, Tohno E, Kamma H, Takahashi H, Shiina T, et al. Breast disease: clinical application of US elastography for diagnosis. Radiology 2006; 239: 341-50. [CrossRef]
20. Choi YJ, Lee JH, Baek JH. Ultrasound elastography for evaluation of cervical lymph nodes. Ultrasonography 2015; 34: 157-64. [CrossRef]
21. Schmitt CP, Shroff R. Disorder of bone mineral metabolism in chronic kidney disease. Geary DF, Schaefer F eds. Pediatric Kidney Disease. 2nd edn. Springer-Verlag Berlin Heidelberg. 2008; pp. 1533-66. [CrossRef]
22. Bakkaloglu SA, Wesseling-Perry K, Pereira RC, Gales B, Wang HJ, Elashoff RM, et al. Value of the new bone classification system in pediatric renal osteodystrophy. Clin J Am Soc Nephrol 2010; 5: 1860-6. [CrossRef]
23. K-DIGO Disease: Improving Global Outcomes (KDIGO) CKD-MBD Work Group. KDIGO clinical practice guideline for the diagnosis, evaluation, prevention, and treatment of Chronic Kidney Disease-Mineral and Bone Disorder (CKD-MBD). Kidney Int Suppl 2009; 113: 1-130.
24. Golu I, Sporea I, Moleriu L, Tudor A, Cornianu M, Vlad A, et al. 2D-shear wave elastography in the evaluation of parathyroid lesions in patients with hyperparathyroidism. Int J Endocrinol 2017; 2017: 9092120. [CrossRef]
25. Kiratli PO, Ceylan E, Naldöken S, Beylergil V. Impaired Tc-99 m MIBI uptake in the thyroid and parathyroid glands during early phase imaging in hemodialysis patients. Rev Esp Med Nucl 2004; 23: 347-51. [CrossRef]
26. Chapuis Y, Fulla Y, Bonnichon P, Tarla E, Abboud B, Pitre J, et al. Values of ultrasonography, sestamibi scintigraphy, and intraoperative measurement of 1-84 PTH for unilateral neck exploration of primary hyperparathyroidism. World J Surg 1996; 20: 835-9. [CrossRef]
27. Batur A, Atmaca M, Yavuz A, Ozgökce M, Bora A, Bulut MD, et al. Ultrasound elastography for distinction between parathyroid adenomas and thyroid nodules. J Ultrasound Med 2016; 35: 1277-82. [CrossRef]